Three Distinct Scenarios under Polymer, Surfactant, and Colloidal Interaction

John Philip,* G. Gnanaprakash, T. Jayakumar, P. Kalyanasundaram, and B. Raj

DPEND, Indira Gandhi Centre for Atomic Research, Kalpakkam 603 102, India

Received February 28, 2003; Revised Manuscript Received July 24, 2003

ABSTRACT: Force measurement between emulsion droplets in the presence of a neutral polymer, poly(vinyl alcohol), and an ionic surfactant, sodium dodecyl sulfate, reveals that the interaction between polymer, surfactant, and colloid can lead to three distinct scenarios, depending on the sequence of adsorption of polymer and surfactant onto the colloidal interface. In the first two cases, where the colloidal interface is adsorbed with or without surfactant molecules, polymer−surfactant complexation occurs in the bulk phase but without being adsorbed at the interface. Under the above condition, the repulsive force between colloidal droplets is not significantly altered by polymer−surfactant complexes. In the third case, where the polymer is preadsorbed at the colloidal interface, polymer−surfactant interaction leads to dramatic changes in repulsive forces due to conformational changes of polymers at the interface, enhancing the stability of the colloid considerably.

Introduction

The ability of polymer−surfactant complexes to alter rheological properties and stability of colloidal formulations has been exploited in various industrial products such as paints, detergents, cosmetics, pharmaceuticals, etc. There is a considerable amount of literature on the topic of polymer−surfactant interaction, and we list only a few articles that are relevant to the context of this work.[1−38] Most of the investigations on associative behavior deal with interactions between polymer and surfactant molecules in bulk solutions.[1−21] Surprisingly, the effect of polymer−surfactant interactions on colloidal stability has been investigated sparsely, though it has tremendous technological importance, probably due to lack of effective experimental tools. There are a few studies on the effect of force between two mica surfaces, under the influence of polymer−surfactant interactions.[22−27] However, polymer−surfactant interactions in the presence of colloids can be much more complicated. Three different situations can exist, depending upon the nature of polymer, the interface, and the surfactant.[28−33] In the first case, the polymer and surfactant are noncomplexing but both adsorb at the interface, where there will be competition for surface sites. (Another possible scenario in the above case is that one of the species may adsorb at the interface.) In the second case, the polymer and surfactant form a complex but only one adsorb at the interface. The nonadsorbing species may complex with the adsorbed species, thus becoming effectively attached to the interface. There may be a competition between the adsorbed surfactant−polymer complexes and solution complexes. In the third case, both polymer and the surfactant adsorb at the interface and form solution complexes. Thus, they may adsorb as a complex directly from solution and adsorb individually. Here, competition may exist between surfactant, polymer, and the complex for adsorption.

Although there are number of studies on the associative nature of polymers in bulk solutions,[1−21] solid interfaces,[28−38] and air−water interface,[18,36] there are no reports on the effect of surfactant interaction with a polymer, which is already adsorbed at a liquid−liquid interface such as emulsions. Earlier, Chari et al.[18] have made an attempt to understand the sequential adsorption behavior of polymer and surfactants in bulk solutions, that is in equilibrium with colloidal particles, to obtain insight into the stability toward Oswald ripening, solvent-mediated phase transformation, and the interplay between polymer−surfactant interaction. They have used ESR and equilibrium dialysis methods to probe the stability aspects. However, it must be noted that the destabilization mechanism, in the present system, is mainly due to Brownian coagulation and coalescence mechanisms due to poorly miscible nature of octane and water. Compared to the classical approach of assessing the stability of a colloidal system by visually observing the settling of the colloidal formulation, the force measurement tool utilized in our experiment is a unique and robust approach which provides valuable insights into the association phenomena (e.g., exact values of decay length, radius of gyration of the adsorbed polymers (R_g), first interaction length where the tails begin to overlap, magnitude of force, etc.).

Since the interplay of forces acting between the colloidal particles determines the stability of colloidal systems, an understanding of the nature of forces existing between colloidal particles is challenging from both a fundamental point of view and practical consideration to tailor colloidal formulations with long-term stability. Using a new force measurement approach,[39−41] we have been successful in investigating the role of associative polymers on colloidal forces in the presence of ionic and nonionic surfactants. Especially, our experimental tool has been very effective in obtaining insight into the very early stages of polymer−surfactant−colloidal interaction, i.e., much below the critical aggregation concentration (cac). Recently, we have investigated the third scenario, i.e., the effect of surfactant interaction with a polymer that is already adsorbed at an oil-in-water interface and its influence on colloidal forces.[41−43] These investigations reveal that neutral polymer layers, already adsorbed at an oil-in-water interface, undergo a stretching due to its interac-

* To whom correspondences should be addressed. E-mail philip@igcar.ernet.in.

10.1021/ma0342628 CCC: $25.00
Published on Web 10/31/2003

tion with surfactants. Upon stretching, the first interaction length follows a power law dependence on surfactant concentration.[42] As a continuation of the above work, we investigate the effect of polymer−surfactant interaction on repulsive forces where the colloidal particles are (I) preadsorbed with surfactant molecules, (II) barely covered with surfactant molecules, and (III) preadsorbed with polymer.

Experimental Section

Materials. Colloidal formulation used in the experiments was a direct emulsion (i.e., oil-in-water) of ferrofluid. The ferrofluid oil consists of a collection of ferromagnetic domains of Fe_2O_3, of about 10 nm size, dispersed in a continuous phase of octane. Monodispersed emulsions with narrow size distributions were obtained using the fractionation technique.[44] When surfactant concentration is above a critical micellar concentration, emulsions droplets begin to flocculate due to depletion flocculation induced by nonadsorbed surfactant. As emulsion droplets approach closer, the thickness of the continuous phase film becomes smaller and smaller, and when it is smaller than the micelle diameter, micelles are expelled from the thin film. Therefore, the thin film region experiences a larger activity of the solvent than the surrounding, and an osmotic pressure develops, pushing the droplets closer. On addition of surfactant to a critical concentration to a typical polydispersed O/W emulsion, the dense phase of aggregated oil droplets separates from a dilute phase of free droplets. At the flocculation threshold, the dense phase contains most of the bigger droplets and the dilute phase mainly smaller ones. In the first step, the dilute phase is separated, and the dense phase is again diluted with more surfactant. The above process is repeated several times to obtain monodisperesed emulsion. Monodispersed oil-in-water emulsions with droplet diameter of about 194 nm have been used in our studies. The surfactant used in our experiment, sodium dodecyl sulfate (SDS), was obtained from Sigma. The polymer used in the studies was a statistical copolymer of vinyl alcohol (88%) and vinyl acetate (vac-12%), which is randomly distributed along the polymer chain with average molecular weight of 155 000 units (155K). The unperturbed radius of gyration of the free polymer (R_g) was obtained from dynamic light scattering and viscometric measurements. The polymer concentration used in all our experiments was 0.6 wt %. Triply distilled water filtered with a 0.22 μm Millipore filter was used. The size distribution of the final emulsion has been measured by using a Malvern Instruments master sizer. An optical phase contrast microscope (M/s Leica DM IRM, Germany) equipped with a digital camera (JVC) and imaging software (Leica) has been used for micromanipulation of the emulsion droplets.

Methods: Force Measurement. Details of the force measurement experimental procedure were described in earlier publications.[39−41] Because of the superparamagnetic nature of ferrofluid droplets, they form chains when subjected to an applied field because of induced magnetic dipole in each droplet. The magnitude of the induced dipole is controlled by the strength of the applied magnetic field. At low concentration, one droplet thick chains are well separated and oriented along the field direction. Because of the presence of the one-dimensional ordered structure, a Bragg peak appears, from which the interdroplet separation (h) has been measured precisely using a spectrograph. The condition for forming a linear chain is that the repulsive force between the droplets must exactly balance the attractive force between the droplets induced by the applied magnetic field. The attractive dipole force within an infinitely long chain is[45]

$$F_{\text{chain}} = -\sum_{n=1}^{\infty} n \frac{6m^2}{(nd)^4} = -\frac{1.202}{2\pi\mu_0}\frac{3m^2}{d^4} \qquad (1)$$

Here, m is the induced magnetic moment of each droplet, which can be determined self-consistently from the intrinsic susceptibility of the ferrofluid, spherical shape of the drop, and presence of neighboring drops.

$$m = 4\mu_0\pi a^3\chi_s H_T/3 \qquad (2)$$

Here, μ_0 is the magnetic permeability of free space and H_T is the total magnetic field acting on each drop. It must be noted that the formula used in the force calculation assumes a spherical shape for the droplets. Because of strong surface tension, the elongation of the nanometer-sized droplet can be very small. According to a calculation,[45] for a ferrofluid droplet of radius (r_0) equal to 100 nm, at a magnetic field strength of 250 Oe, the eccentricity value is about 1.3×10^{-3}. This corresponds to the major axis "a" = $((1-4) \times 10^{-4})r_0$ and the minor axis "b" = $((1-2) \times 10^{-4})r_0$. Therefore, it is evident that the elongation of the droplet is negligible in the field strength (force) used in our experiments.

The sensitivity in the distance measurement in our experimental setup was 0.1 nm. The range of force that can be probed using this technique is $10^{-11}-10^{-13}$ N. Compared to the surface force apparatus,[46,47] where the force is measured between two mica surfaces, we probe relatively weak forces existing between individual nanometer-sized colloidal particles. To study the effect of polymer adsorption on the force profiles, the emulsion is washed with PVA or surfactant solution for about 4−5 times and then incubated for about 72 h. No significant variations in the force profiles were noticed under these conditions. For association experiments, the required quantity of surfactants is added to the incubated emulsion, and the force measurements have been performed at 23 °C.

Experimental Results and Discussion

From the force profile, we deduce the decay length (λ) from the slope and the first interaction length or onset of repulsion ($2L_0$) defined as the distance at which the magnitude of force is 2×10^{-13} N. What is measured by this technique is the repulsive forces between the individual emulsion droplets as a function of distance between them. For the sake of clarity, we first discuss the nature of the force profiles when the colloidal suspension is stabilized with surfactant and polymers independently.

For a surfactant stabilized colloids, the electrostatic double-layer force profiles decays roughly exponentially with a characteristic length called the Debye length κ, i.e., $F(h) \approx \psi_0 \exp(-\kappa h)$. Here, the magnitude of force is governed by the surface potential.[39−41,47−50] The inverse Debye length (κ^{-1}) essentially depends on the electrolyte concentration (C_s) and can be represented as[46,47]

$$\kappa^{-1} = \left[\left(\frac{4\pi q^2}{\epsilon kT}\right)2C_s\right]^{-0.5} \qquad (3)$$

where "q" is the charge, kT is the thermal energy, and ϵ is the dielectric permittivity of the suspending medium. Recent studies on force profiles between two mica surfaces, using surface force apparatus, in the presence of monovalent electrolytes also found excellent agreement between the experimental and theoretically predicted values of the Debye length.[50,51] However, electrostatic screening length in solutions of multivalent electrolytes shows deviations from theoretical predictions.[49]

Measurement of forces between emulsion droplets in the presence of ionic surfactants shows that the experimental slopes of the force profiles for different surfactant concentrations are in good agreement with the theoretical predictions.[39−41] The surface potential values obtained from the best fit on the force profiles were also

found to be in very good agreement with those obtained independently from the electrophoresis mobility (e.g., −45 mV for sodium dodecyl sulfate stabilized octane droplets from the best fit against −47 mV from electrophoresis mobility experiment). In the case of nonionic surfactant stabilized droplets, a hard sphere force profile at close contact (interdroplet spacing $h = 0$) and the observed diameter of droplet ($2a = \lambda_0/2n$) were in reasonable agreement with that obtained from light scattering experiments.[40] Therefore, both magnitude and decay length, obtained from the force profiles, compare very well with theoretical predictions in simple model systems.

The main contributions to the interaction free energy for two colloidal particles, covered with polymers, approaching each other are originating from the loss of configurational entropy of the polymer and the excluded-volume interaction. The force profiles in the presence of adsorbed polymers and weak polyelectrolytes decay exponentially with a characteristic length proportional to the radius of gyration.[51,52]

$$F(h) = k \exp\left(\frac{-h}{\lambda}\right) \tag{4}$$

where "h" is the interdroplet spacing and "λ" is the decay length. These observations were consistent with the theoretical predictions obtained using both a mean field and a scaling approach.[53,54] The theory distinguishes the loops and tail sections of the adsorbed chains and involves three length scales: the adsorbed layer thickness λ, an adsorption length z^* that separates the regions where the monomer concentration is dominated by loops and by tails, and a microscopic length "b" inversely proportional to the adsorption strength. The experimentally observed decay length values for polymers (PVA-vac) and polyelectrolytes (PAA) of different molecular weights were in good agreement with the R_g values obtained from light scattering and viscometry. For example, for PVA of molecular weight 40 000 and 155 000, the characteristic decay length values obtained from the force profile were about 6 and 16 nm, respectively, and are in good agreement with the hydrodynamic radius of 6.4 and 16.5 nm obtained from our viscometric and light scattering measurements. Our experimental studies on a variety of polymers and polyelectrolytes of different molecular weights show that the decay length values are comparable to the unperturbed radius of gyration. Recent investigations using optical tweezers[55] on micron-sized silica spheres adsorbed with polymers also found a similar exponential decay length proportional to the radius of gyration, in agreement with both mean field and a scaling theory ($\lambda \approx 0.6R_g$). Though the magnitude of force and the distance ranges in the above two cases are significantly different, the correlation between the decay length and radius of gyration was remarkable. Therefore, the force measurement experimental technique has been established as a powerful tool to study the electrostatic, steric, and electrosteric interactions between emulsion droplets. It also gives accurate values of Debye length and surface potentials for charge-stabilized colloids and unperturbed radius of gyration of the polymer adsorbed at the interface.

First, we discuss the results of case I where emulsion is initially stabilized with SDS at 8 mM (cmc). Into the above system, polymer concentration is increased systematically. The repulsive force as a function of distance

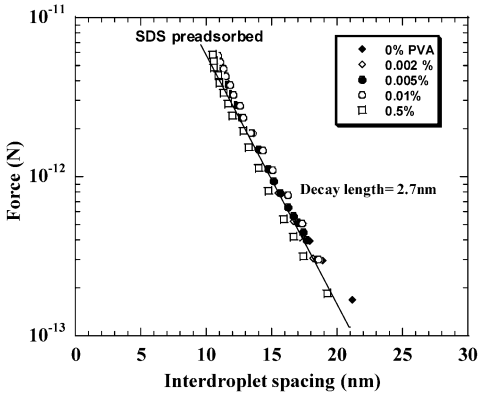

Figure 1. Forces between the ferrofluid droplets, preadsorbed with sodium dodecyl sulfate (SDS) at 8 mM (case I), as a function of distance, for various PVA concentrations: 0, 0.002, 0.005, 0.01, and 0.5 wt %. The solid line represents the average value of the best fit, where the average decay length is about 2.7 nm.

between the ferrofluid droplets, stabilized with SDS at 8 mM concentration, is shown in Figure 1 (marked as 0% PVA). Slowly we introduce PVA of different concentrations varying from 0.002, 0.005, 0.01, and 0.5% to study the effect of polymer−surfactant complexation on force profiles. After each addition, the emulsion is incubated for over 48 h for reaching the equilibrium. It can be seen that the force profiles remain almost the same as in the case of 0% PVA. The average decay length for these curves was found to be 2.7 nm and is shown by the solid line. In the above case, it is obvious that the bulk aqueous fluid contains surfactant molecules (free) in equilibrium with micelles. As the effective concentration is above cmc, the interface must be fully covered by surfactant molecules, and the expected decay length under the above condition is 3.4 nm. The experimental value of the decay length obtained from the force profile, 2.9 nm, is in good agreement with the predicted value. When polymer is introduced into the solution, some micelles from the bulk will associate or bind with the polymer coil and remain in equilibrium with the free micelles and excess polymers (depicted in Figure 8). At the cmc of SDS, the interface of emulsion droplets must be fully covered with surfactant molecules and correspond to the plateau of the adsorption curve. When the emulsion is preadsorbed with surfactant molecules, the introduction of polymer did not influence the force profile significantly. If there was adsorption of polymer or polymer−surfactant complexes at the emulsion interface, the decay length would have been increased to a value close to the unperturbed radius of gyration of the PVA, which was around 16 nm. However, the decay length variation for the PVA concentration range of 0.001−0.5 wt % was 2.93−2.51 nm, and the corresponding $2L_0$ values were 20.4 and 18.6 nm, respectively. Both the decay length and the $2L_0$ values, with varying polymer concentration, are plotted in Figure 2. Neither the decay length nor the $2L_0$ values vary significantly with increasing polymer concentration.

Figure 3 shows the force distance profile for an emulsion very weakly charged (stabilized with SDS at a concentration of 0.27 mM or cmc/30). Polymer and surfactant were premixed separately and later added to the emulsion. In all these cases, the polymer concentration was fixed at 0.6 wt %. Premixed polymer−surfactant mixture was incubated sufficiently (>2 h)

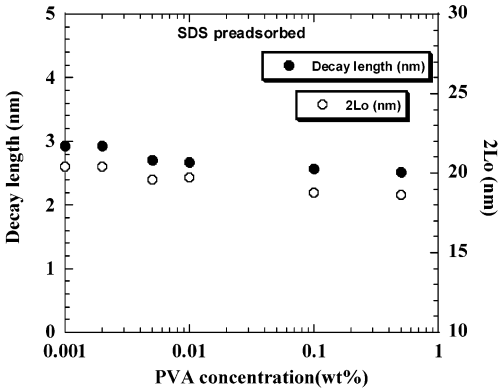

Figure 2. Decay length (λ) and first interaction length ($2L_0$) values deduced from the force curves in Figure 1 as a function of polymer concentrations. Emulsion used in the above case was stabilized with SDS at 8 mM.

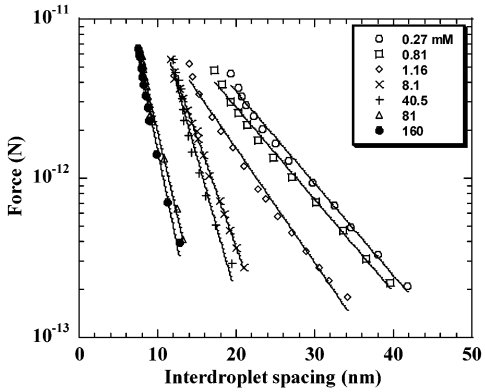

Figure 3. Force profiles for different SDS concentrations (case II), where premixed PVA−SDS was added to the emulsion. In all the cases, the polymer concentration was 0.6 wt %. The surfactant concentrations were 0.27, 0.81, 1.16, 8.1, 40.5, 81, and 160 mM. The best fits, using eq 4, are shown by the solid lines.

before adding to the emulsion. The force profiles are again repulsive and exponentially decaying with a characteristic decay length comparable to the Debye lengths, corresponding to the equivalent amount of surfactant concentration present in the premixed system. The values of the decay length obtained from the force profiles for surfactant concentrations 0.27, 0.81, 1.16, 2.7, 8.1, 40.5, 81, and 160 mM were 7.52 (18.9), 7.5 (10.9), 6 (9.1), 4 (6.0), 3 (3.4), 2.5 (2.8), 2.1 (2.3), and 1.86 (1.9) nm, respectively. The theoretical values of Debye length for equivalent surfactant concentrations are given in parenthese. The first interaction length dropped from 42 to 14 nm over the above concentration range. This shows that although polymer−surfactant complexes are formed in the bulk solution, the excess surfactant molecules have an affinity to adsorb at droplet interface. Here, neither the polymer nor the polymer−surfactant complexes are adsorbed at the emulsion interface.

For case III, where the polymer is preadsorbed at the emulsion droplet interface, the force profiles are shown in Figure 4. The force profile in the absence of any surfactant is the reference curve (0 mM). The polymer concentration in all the curves was 0.6 wt %, corresponding to the plateau in the adsorption isotherm (1.5−2 mg/m^2 for the oil−water interface).[51,56] The force profiles are repulsive and exponentially decaying with a characteristic decay length comparable to the R_g of

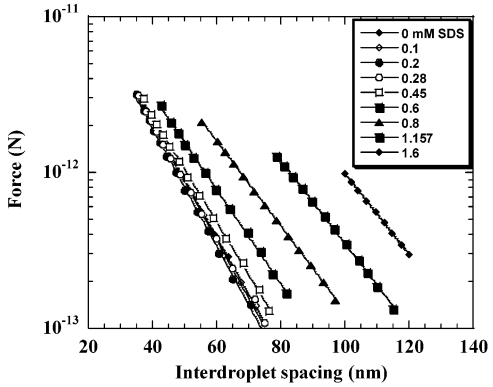

Figure 4. Force profiles for different SDS concentrations (case III), where PVA is preadsorbed on emulsion droplets. In all the cases, the polymer concentration was fixed at 0.6 wt %. The surfactant concentrations were 0.1, 0.2, 0.28, 0.45, 0.6, 0.8, 1.157, and 1.6 mM. The best fits, using eq 4, are shown by the solid lines.

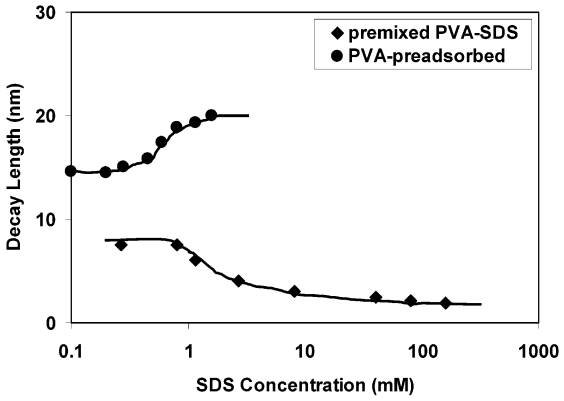

Figure 5. Decay length, values deduced from the force curves in Figures 3 and 4, as a function of surfactant concentrations. Solid line is a guide to the eye.

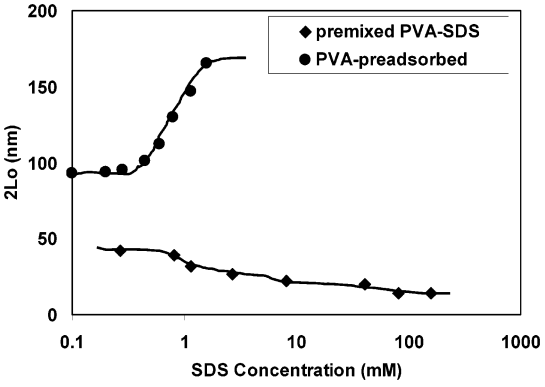

Figure 6. First interaction length ($2L_0$) values deduced from the force curves in Figures 3 and 4 as a function of surfactant concentration. Solid line is a guide to the eye.

free polymer (16 nm). As the concentration of the surfactant increases, the decay length and the onset of repulsion increase. Here, the SDS concentration was varied from 0.1 to 1.6 mM. Beyond 1.6 mM, we were not able to measure the Bragg peak (and hence the interdroplet spacing h) due to poor reflectivity from the samples. The variations of the experimentally obtained decay length and $2L_0$ values for case II and case III are shown in Figures 5 and 6, respectively. In case II, both decay length and $2L_0$ values decrease with increasing surfactant concentration, while under case III, both the

values increase with surfactant concentration, beyond some surfactant concentration. The decay length values for the surfactant concentrations 0.1, 0.2, 0.28, 0.45, 0.6, 0.8, 1.157, and 1.6 mM were 14.6, 14.5, 15, 15.8, 17.37, 18.9, 19, and 19.9 nm, respectively. It can be seen that the $2L_0$ value has increased from 93 to 165 nm when the surfactant concentration was changed from 0.1 to 1.6 mM. Though we were not able to increase the surfactant concentration up to the saturation levels, we have been able to see the saturation points clearly for polymers of low molecular weights (40K and 115K).[42,43] These results indicate that there is no desorption of the polymer from the droplet interface, with increasing surfactant concentration, in case III. These results show that the interaction between the surfactant and preadsorbed polymer drastically changes polymer conformation at the interface and hence the repulsive forces, especially the onset of repulsion. The polymer−surfactant interaction leads to changes in the hydrophobic−hydrophilic balance of the polymer coil, which causes conformational changes in the polymer coil. Though the experimental decay lengths increases marginally with increasing surfactant concentrations, the magnitude of increase was not significant compared to the increase of $2L_0$ values.

Small-angle neutron scattering (SANS) results[33] on polystyrene latex preadsorbed with gelatin showed that the adsorption of gelatin on the latex particle increases with SDS up to a concentration range of 2−4 mM. Further increase in the SDS leads to saturation at around 16 mM, corresponding to a maximum expansion of gelatin layer due to saturation in the inter- and intrachain repulsion. Although the nature of interface in the above experiment is very much different from our case (i.e., negatively charged polystyrene−water interface adsorbed with polyampholyte gelatin), we could also see a saturation in the decay length at higher surfactant concentration (about 4.0 mM SDS at a concentration of 0.45 wt %). In the case of PVA at lower molecular weights (40K) the saturation occurs at a surfactant concentration of 8 mM.[42,43] Though desorption of adsorbed complexes (gelatin−SDS) from the polystyrene at very high concentrations of SDS (≫cmc) was observed, such desorption was not evident from the force profiles in the case of emulsion droplets, probably due to lower surfactant concentrations used in our experiments. The force profiles were remarkably reproducible in the presence of polymer−surfactant complexes over a period of more than 12 months, indicating equilibrium in the adsorption characteristics (Figure 7). In the presence of polymer alone, the force profiles often show slight hysteresis with time. However, no such hysteresis has been observed under associating conditions.

It is well-known that the critical aggregation concentration (cac) values vary with the nature of surfactants (alkyl chain length, headgroup, charge density, etc.). But the question here is whether the cac values are the same in the case of two-component (polymer−surfactant) and three-component systems (polymer−surfactant−colloid). We have measured the cac values in bulk solutions (without emulsion) using conductivity and viscometry, and values in the bulk solution for SDS− PVA system were about 2.9.mM (for 155K) and 4.3 mM (for 40K). However, the force experiments with three-component system show that the onset of repulsion begins at surfactant concentrations of 0.12 and 0.16 mM for 155K and 40K, respectively. We must note that the repulsive

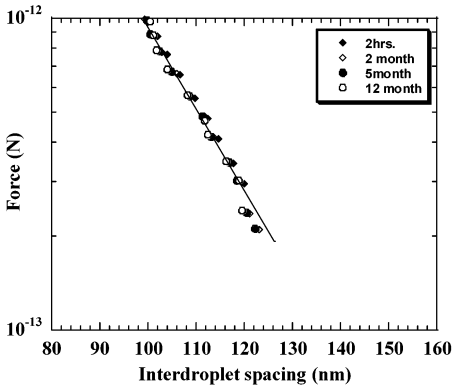

Figure 7. Force−distance profiles for PVA 155-SDS stabilized emulsion at various intervals of time. The polymer concentration was 0.65 wt %, and the surfactant concentration was 1.6 mM. The solid line shows the exponential fit (eq 4).

force profile measured here is due to steric interaction between colloidal particles covered with polymers and not due to the interaction between polymer−surfactant complexes in the bulk. This shows that the onset of repulsion we measure from the force profile is highly sensitive to the association phenomena. These experimental observations suggest that in the case of three component systems one needs to simultaneously examine what happens to the polymer at the interface and those in the bulk during the association process. This also suggests that the critical concentrations at which the association occurs for the adsorbed polymer and the free polymer in the bulk solution could be different.

In contrast to our force measurement and SANS[33] results, surface force measurements on the association between a low charge density polyelectrolyte, adsorbed onto negatively charged mica (and silica) surfaces, and sodium dodecyl sulfate show considerable reduction of the repulsive forces as the surfactant concentration is increased.[26] It has been found that the onset of repulsion ($2L_0$) was decreased from 80 to about 40 nm when the SDS concentration is increased from 0 to 2 mM, due to desorption of the polyelectrolyte at higher surfactant concentrations. These experimental results clearly show that the adsorption at the interface depends on the sequence or conditions at which the surfactant and polymer are introduced into the colloidal formulations. Recent neutron reflectivity studies,[6] to determine the adsorbed amount of surfactants at the interfaces in multicomponent systems, also reveal that the adsorption at the interface depends on the competition between the complex formation in the bulk and at the interface.

On the basis of the above experimental findings, the expected conformations of polymer−surfactant complexes at the oil−water interface are depicted in Figure 8a−c. In case I, the added polymer associates with excess surfactants present in the bulk solution, but the complexes prefer to remain in the bulk phase. Alternately, the polymer−surfactant complexes are unable to displace the bound surfactant molecules from the liquid−liquid interface. Irrespective of the amount of polymer−surfactant concentration in the bulk, the experimental decay length values (2.7 nm) remain comparable to the Debye lengths (3.4 nm), corresponding to the concentration of ion species in the bulk solution (eq 3). This means that the force profile is dictated by the double-layer forces due to adsorbed surfactant molecules. In case II, the decay length decreases with increasing surfactant concentration.

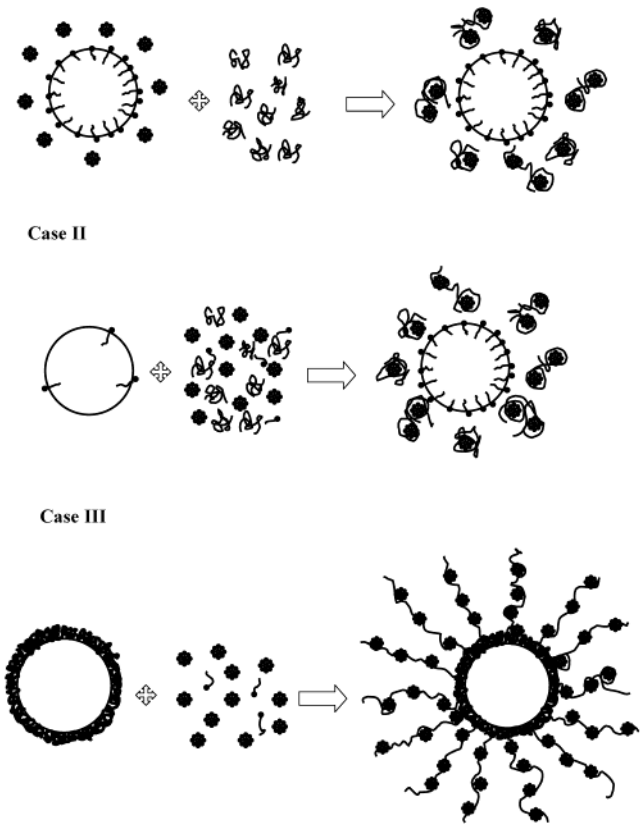

Figure 8. Schematic diagram of polymer−surfactant complex on emulsion droplets for cases I, II, and III. The stretching shown in case III is slightly exaggerated.

Above some surfactant concentration (i.e., above 8 mM SDS), the decay length almost coincides with the Debye length, indicating that the droplet interface is fully adsorbed with surfactant molecules. This shows that polymer−surfactant complexes remain in the bulk solution. In case III, the initial decay length values (≈15.0 nm) correspond to the R_g value of the PVA, indicating that the polymer is adsorbed at the oil−water interface. As the concentration of SDS increases, it interacts with the adsorbed polymer tails, leading to conformational changes of the adsorbed polymer. We believe that the ionic surfactants are bound to the sparsely covered "distal regime" which is further stretched by surfactant molecules or micelles. As the concentration increases, more and more surfactant molecules and micelles go into the folded chains (central regime) that stretch more loops further. Therefore, at higher surfactant concentrations, the neutral polymer chains at the interface are likely to adopt diblock polyelectrolyte type conformations on the emulsion droplet, with one block (hydrophobic-vac) anchored at the oil interface and the other block (hydrophilic-PVA) with adsorbed micelles, stretched out in the continuous phase. Here, the charges on the chain repel each other, and the electrostatic repulsion collectively lead to chain stretching on length scales larger than the electrostatic blob size.[57,58] The stretching is expected to continue until the coils are saturated with adsorbed surfactant micelles. Finally, these experimental findings reveal that the polymer−surfactant complexation results originating from various experimental techniques can be compared only if the sequence of adsorption and experimental conditions are similar.

Concerning the generality, we have studied the force measurements using polymers of three different molecular weights (40K, 115K, 155K), four surfactants (cationic, anionic, and nonionic), and emulsions made of different oils. In all those cases, we could observe the same phenomena. More careful experiments like SANS may bring new insights into this rather "intriguing" stretching phenomena.

Conclusions

Systematic force measurements between emulsion droplets in the presence of neutral polymer and surfactant reveal that the polymer−surfactant can lead to three distinct scenarios, depending on the sequence of adsorption of polymer or surfactant onto the colloid. The stability of the colloid can be enhanced only if the polymer is preadsorbed on the colloids, before the polymer−surfactant complexation is initiated. Under the above condition, the polymer−surfactant interaction leads to dramatic changes in the repulsive forces due to conformational changes of the polymer at the interface. The adsorption at an interface depends on the competition between the complex formation in the bulk and at the interface. Finally, the new experimental findings provide the right conditions at which the polymer−surfactant complexation can enhance the stability of the colloidal suspension significantly and the role of sequential adsorption of polymer, surfactant, and colloid on repulsive forces.

Acknowledgment. The authors thank Mr. S. B. Bhoje, Director, IGCAR, for his interest and support for this research program and Dr. S. L. Mannan, Associate Director, MDG, for encouragements. Support from Indo-French Centre for Promotion of Advanced Scientific Research (IFCPAR), New Delhi, is greatly acknowledged. J.P. thanks O. Mondain Monval, Leal Calderon, and J. Bibette for initiating the Indo-French cooperation.

References and Notes

(1) *Interactions of Surfactants with Polymers and Proteins;* Goddard, E. D., Anadapadmanabhan, K. P., Eds.; CRC Press: Boca Raton, FL, 1993.
(2) *Polymer-Surfactant System*; Kwak, J. C. T., Ed.; Marcel Dekker: NewYork, 1998.
(3) Armentrout, R. S.; McCormick, C. L. *Macromolecules* **2000**, *33*, 419−424.
(4) Smith, G. L.; McCormick, C. L. *Langmuir* **2001**, *17*, 1719−1725 (see the articles published by this group under the title water-soluble polymers).
(5) Purcell, I. P.; Lu, J. R.; Thomas, R. K.; Howe, A. M.; Penfold, J. *Langmuir* **1998**, *14*, 1637−1645.
(6) Staples, E.; Tucker, I.; Penfold, J.; Warren, N.; Thomas, R. K. *J. Phys.: Condens. Matter* **2000**, *12*, 6023−6038; *Langmuir* **2002**, *18*, 5139−5146; *Langmuir* **2002**, *18*, 5147−5153.
(7) Diamant, H.; Andelman, D. *Macromolecules* **2000**, *33*, 8050−8061.
(8) Cabane, B. *J. Phys. Chem.* **1977**, *81*, 1639−1645; *J. Phys. (Paris)* **1982**, *43*, 1529−1542; *Colliods Surf.* **1985**, *13*, 19−33. Lee, L. T.; Cabane, B. *Macromolecules* **1997**, *30*, 6559−6566.
(9) Nikas, Y. J.; Blankschtein, D. *Langmuir* **1994**, *10*, 3512−3528.
(10) Ruckenstein, E. *Langmuir* **1999**, *15*, 8086−3528.
(11) Antony, O.; Zana, R. *Langmuir* **1994**, *10*, 4048−4052; *Langmuir* **1996**, *12*, 3590−3597; *Langmuir* **1996**, *12*, 1967−1975.
(12) Winnik, M. A.; Yekta, A. *Curr. Opin. Colloid Interface Sci.* **1997**, *2*, 424−429. Mangy, B.; Iliopoulos, I.; Audebert, I.; Piculell, R.; Lindman, L. B. *Prog. Colloid Polym. Sci.* **1992**, *89*, 118−127.
(13) Hoff, E.; Nystrom, B.; Lindman, B. *Lamgmuir* **2001**, *17*, 28−34.
(14) Xia, J.; Dublin, P. L.; Kim, Y. *J. Phys. Chem.* **1992**, *96*, 6805−6811.

(15) Heitz, C.; Prud'homme, R. K.; Kohn, J. *Macromolecules* **1999**, *32*, 6658−6667.
(16) Lee, L. T.; Cabane, B. *Macromolecules* **1997**, *30*, 6559; *Curr. Opin. Colloid Sci.* **1999**, *4*, 205−213 (see this reference for a comprehensive review on SANS studies on polymer−surfactant mixtures).
(17) Sjostrom, J.; Piculell, L. *Langmuir* **2001**, *17*, 3836−3843.
(18) Chari, K.; Hossain, T. *J. Phys. Chem.* **1991**, *95*, 3302−3308. Chari, K.; Antalek, B.; Kowalczyk, J.; Eachus, R. S.; Chen, T. *J. Phys. Chem. B* **1999**, *103*, 9867−9872. Dhara, D.; Shah, D. O. *J. Phys. Chem. B* **2001**, *5*, 61−66.
(19) Zhu, P. W.; Napper, D. H. *Phys. Rev. E* **2000**, *61*, 2859−2863; *Phys. Rev. E* **2000**, *61*, 6866−6871.
(20) Folmer, B. M.; Kronberg, B. *Langmuir* **2000**, *16*, 5987−5992.
(21) Robb, I. D.; Stevenson, P. *Langmuir* **2000**, *16*, 7168−7172.
(22) Claesson, P. M.; Blomberg, E.; Paulson, O.; Malmsten, M. *Colloid Surf. A: Physicochem., Eng. Aspects* **1996**, *112*, 131−139.
(23) Kim, H. S.; Lau, W.; Kumacheva, E. *Macromolecules* **2000**, *33*, 4561−4567. Fielden, M. L.; Claesson, P. M.; Schillen, K. *Langmuir* **1998**, *14*, 5366−5375.
(24) Zhang, K.; Jonstromer, J.; Lindman, B. *Colloids Surf., A* **1994**, *87*, 133−142.
(25) Kjellim, U. R. M.; Claesson, P. M.; Audebert, R. *J. Colloid Interface Sci.* **1997**, *190*, 476−486.
(26) Rojas, O. J.; Neuman, R. D.; Claesson, P. M. *J. Colloid Interface Sci.* **2001**, *237*, 104−111.
(27) Bremmele, K. E.; Jameson, G. J.; Biggs, S. *Colloids Surf., A* **1999**, *155*, 1−10.
(28) Wesley, R. D.; Cosgrove, T.; Thompson, L. *Langmuir* **1999**, *15*, 8376−8382.
(29) Ghodbane, J.; Denoyel, R. *Colloids Surf. A* **1997**, *127*, 97−104.
(30) Bury, R.; Desmazieres, B.; Treiner, C. *Colloids Surf., A* **1997**, *127*, 113−124.
(31) Otsuka, H.; Esumi, K.; Ring, T. A.; Li, J. T.; Caldwell, K. D. *Colloids Surf., A* **1996**, *116*, 161−171.
(32) Cosgrove, T.; Mears, S.; Thompson, J. L.; Howell, I. *ACS Symp. Ser.* **1995**, *No. 615*, 196−203.
(33) Marshall, J. C.; Cosgrove, T.; Howe, A.; Jack, K. *Langmuir* **2002**, *18*, 9668−9675.
(34) Braem, A. D.; Prieve, D. C.; Tilton, R. D. *Langmuir* **2001**, *17*, 883−890.
(35) Pagac, E. S.; Prieve, D. C.; Tilton, R. D. *Langmuir* **1998**, *14*, 2333−2342.
(36) Sun, M. L.; Tilton, R. D. *Colloids Surf., B* **2001**, *20*, 281−293.
(37) Velegol, S. B.; Tilton, R. D. *Langmuir* **2001**, *17*, 219−227.
(38) Furst, E. M.; Pagac, E. S.; Tilton, R. D. *Ind. Eng. Chem. Res.* **1996**, *35*, 1566−1574.
(39) Calderon, F. L.; Stora, T.; Mondain Monval, O.; Bibette, J. *Phys. Rev. Lett.* **1994**, *72*, 2959−2962.
(40) Philip, J.; Mondain Monval, O.; Leal Calderon, F.; Bibette, J. *J. Phys. D: Appl. Phys.* **1997**, *30*, 2798−2803; *Bull. Mater. Sci.* **1999**, *22*, 101−108.
(41) Philip, J.; Jaykumar, T.; Kalynasundaram, P.; Raj, B.; Mondain Monval, O. *Phys. Rev.* **2002**, *66*, 011406-1-7.
(42) Philip, J.; Prakash, G. G.; Jaykumar, T.; Kalynasundaram, P.; Raj, B. *Phys. Rev. Lett.* **2002**, *89*, 268301-1-4.
(43) Philip, J.; Prakash, G. G.; Jaykumar, T.; Kalynasundaram, P.; Mondain Monval, O.; Raj, B. *Langmuir* **2002**, *18*, 4625−4632.
(44) Bibette, J. *J. Colloid Interface Sci.* **1991**, *147*, 474−478.
(45) Zhang, H.; Widom, M. *Phys. Rev. E* **1995**, *51*, 2099−2103.
(46) Isrelachvili, J. N.; Adams, G. E. *J Chem. Soc., Faraday Trans. 1* **1978**, *74*, 975−1001.
(47) Isrelachvili, J. N. *Intermolecular and Surface Forces;* Academic Press: San Diego, CA, 1985.
(48) Pashely, R. M.; Ninham, B. W. *J. Phys. Chem.* **1987**, *91*, 2902−2904.
(49) Kohonen, M. M.; Karaman, M. E.; Pashely, R. M. *Langmuir* **2000**, *16*, 5749−5753.
(50) Tadmor, R.; Hernandez, E.; Chen, N.; Pincus, P.; Isrealachvili, J. N. *Macromolecules* **2002**, *35*, 2380−2388.
(51) Mondain Monval, O.; Espert, A.; Omerjee, P.; Bibette, J.; Leal Calderon, F.; Philip, J.; Joanny, J. F. *Phys. Rev. Lett.* **1998**, *80*, 1778−1781; *Phys. Rev. Lett.* **1995**, *75*, 3364−3367.
(52) Espert, A.; Omerjee, P.; Bibette, J.; Leal Calderon, F.; Mondain Monval, O. *Macromolecules* **1998**, *31*, 7023−7029.
(53) Semenov, A. N.; Bonet-Avalos, J.; Johner, A.; Joanny, J. F. *Macromolecules* **1996**, *29*, 2179−2196; *Macromolecules* **1997**, *30*, 1479−1489.
(54) Fleer, G. J.; Van Male, J.; Johner, A. *Macromolecules* **1999**, *32*, 825−844; *Macromolecules* **1999**, *32*, 845−862.
(55) Owen, R. J.; Crocker, J. C.; Verma, R.; Yodh, A. G. *Phys. Rev. E* **2001**, *64*, 011401 1-5.
(56) Fleer, G.; Cohen Stuart, M.; Scheutjens, J.; Cosgrove, T.; Vincent, B. *Polymer at Interfaces;* Chapman and Hall: London, 1993.
(57) Rubinstein, M.; Colby, R. H.; Dobrynin, A. *Phys. Rev. Lett.* **1994**, *73*, 2776−2779. Rubinstein, M.; Semenov, A. N. *Macromolecules* **2001**, *34*, 1058−1068.
(58) Golestanian, R.; Kardar, M.; Liverpool, T. B. *Phys. Rev. Lett.* **1999**, *82*, 4456−4459.

MA0342628